# Proton-proton physics with the ALICE muon spectrometer at the LHC

N. Bastid

# Proton-proton physics with the ALICE muon spectrometer at the LHC

N. Bastid for the ALICE Collaboration*
*LPC Clermont-Ferrand,*
*IN2P3-CNRS and Université Blaise Pascal*
*63177 Aubière Cedex, France*
(Dated: November 1, 2007)

ALICE, the dedicated heavy ion experiment at the LHC, has also an important proton-proton physics program. The ALICE muon spectrometer will be presented and the corresponding physics analysis will be reviewed. A particular emphasis will be placed on heavy flavour measurement.

PACS numbers: 25.75-q, 25.75.Cj, 25.75.Nq

## I. INTRODUCTION

With a nucleus-nucleus center-of-mass energy that will exceed the one reached at RHIC by about a factor 30, the LHC (Large Hadron Collider) will bring new insights in heavy ion physics. One of the most important aspects of this new energy range will be the abundant production of hard probes which could be used, for the first time, as high statistics probes of the medium. ALICE (A Large Ion Collider Experiment), the experiment designed for and devoted to heavy ion physics at the LHC, aims at investigating the properties of strongly interacting matter at extreme energy densities and temperatures where the formation of the Quark Gluon Plasma is expected.

The successful achievement of the heavy ion program requires also the study of proton-proton, proton-nucleus and light nucleus-nucleus systems. Besides providing the necessary baseline for nucleus-nucleus collisions, proton-proton collisions have an intrinsic interest since they allow to test both perturbative and non-perturbative regimes of QCD in a new kinematic region of very low Bjorken-$x$ values. Therefore, the ALICE proton-proton physics program complements the studies of the dedicated proton-proton experiments at the LHC. In particular, ALICE will provide unique information on low transverse momentum ($p_t$) phenomena.

The LHC is scheduled to start to operate in summer 2008 with proton-proton collisions at $\sqrt{s} = 14$ TeV. It will deliver, in nominal conditions, proton beams at $\sqrt{s} = 14$ TeV seven months per year and Pb beams at $\sqrt{s_{NN}} = 5.5$ TeV one month per year. As can be seen from Table I which summarizes the LHC running conditions for the first five years of operation [1], light ion beams are foreseen. Later options will depend on the first physics results.

In the following, an overview of the ALICE apparatus will be given and we will address selected proton-proton physics topics that will be studied with the ALICE muon spectrometer.

TABLE I: Expected nucleon-nucleon center of mass energy ($\sqrt{s_{NN}}$), average luminosity ($< \mathfrak{L} >$) in ALICE and data taking time per year (t). The corresponding geometrical cross sections ($\sigma_{geo}$) are also given.

| System | $\sqrt{s_{NN}}$ (TeV) | $< \mathfrak{L} >$ (cm$^{-2}$ s$^{-1}$) | t (s/year) | $\sigma_{geo}$ (b) |
|---|---|---|---|---|
| p-p | 14 | $3 \cdot 10^{30}$ | $10^7$ | 0.07 |
| Pb-Pb | 5.5 | $5 \cdot 10^{26}$ | $10^6$ | 7.7 |
| Ar-Ar | 6.3 | $5 \cdot 10^{28}$ | $10^6$ | 2.7 |
| p-Pb | 8.8 | $5 \cdot 10^{28}$ | $10^6$ | 1.9 |

## II. THE ALICE MUON SPECTROMETER

The ALICE apparatus [1], presently in its final installation phase, consists of a central barrel ($|\eta| < 0.9$) placed in the L3 magnet delivering a magnetic field of 0.5 T, a forward muon spectrometer and other sub-detectors of smaller acceptance. The central barrel includes the Inner Tracking System, a large Time Projection Chamber, a Transition Radiation Detector for electron identification and a Time of Flight system for the identification of hadrons.

The main aim of the ALICE muon spectrometer [1–4] is the study of heavy flavour production (open heavy flavours and quarkonia) in the (di)muon channel. In addition, the muon spectrometer also allows to investigate the production of weakly interacting probes ($W^{\pm}$ and $Z^0$ bosons) and vector mesons ($\rho$, $\omega$, $\phi$).

The main design criteria are driven by the requirements that the detector should operate in the high multiplicity environment of central Pb-Pb collisions (between 2000 and 8000 charged particles per unit rapidity expected at mid rapidity) and should reach a mass resolution better than 100 MeV/$c^2$ in the $\Upsilon$ mass region in order to resolve the $\Upsilon(1S)$, $\Upsilon(2S)$ and $\Upsilon(3S)$ states. The ALICE muon spectrometer covers the polar angular range $171° < \theta < 178°$ corresponding to a pseudo-rapidity range $-4.0 < \eta < -2.5$ and has full azimuthal acceptance. It is composed of a passive front absorber positioned close to the interaction region and stopping most of hadrons and photons, a small angle absorber, a dipole magnet with a field integral of 3 Tm, five stations of high granularity tracking chambers, a muon filter and

*Electronic address: nicole.bastid@clermont.in2p3.fr

two stations of trigger chambers. The front absorber and the muon filter stop muons with momentum less than 4 GeV/c.

The trigger system allows to reject background muons (from $\pi$ and $K$ decays) by means of a $p_t$ cut on single muons. Low $p_t$ (1 GeV/c) and high $p_t$ (2 GeV/c) trigger cuts have been optimized for the measurement of charmonia and bottomonia, respectively. The expected muon trigger rates in proton-proton mode are displayed in Table II [5]. They should not exceed 1 kHz in order to keep the dead-time of muon event readout to a low value. Such a rate fits the bandwidth of the ALICE muon High Level Trigger which allows to further reduce the permanent storage rate. Simulation results show that single muon rates and dimuon rates fulfil such a requirement, already for the low $p_t$ trigger cut.

TABLE II: Muon trigger rates for p-p collisions at $\sqrt{s} = 14$ TeV and $< \mathfrak{L} > = 3 \cdot 10^{30}$ cm$^{-2}$s$^{-1}$. They are shown for single muons and unlike-sign (US) dimuons and, for different $p_t$ cuts applied at the trigger level. See text for details.

| Trigger rates (Hz) | f $^{p_t>1\ \mathrm{GeV/c}}$ | f $^{p_t>2\ \mathrm{GeV/c}}$ |
|---|---|---|
| single muons | 510 ± 30 | 225 ± 20 |
| US dimuons | 10 ± 5 | 5 ± 3 |

The ALICE muon spectrometer is currently in its final installation phase. A commissioning run will start in December 2007.

## III. HEAVY FLAVOUR PRODUCTION

At the LHC, hard processes will contribute significantly to the total cross section. Expected yields and cross sections of $c\bar{c}$ and $b\bar{b}$ pairs [6, 7], calculated in the framework of perturbative QCD (pQCD) at next-to-leading order (NLO), are reported in Table III for the 5% most central Pb-Pb collisions at $\sqrt{s_{NN}} = 5.5$ TeV and for p-p collisions at $\sqrt{s} = 14$ TeV.

TABLE III: ALICE baseline for heavy quark production cross sections and yields in p-p collisions ($\sqrt{s} = 14$ TeV) and in central Pb-Pb collisions ($\sqrt{s_{NN}} = 5.5$ TeV). For Pb-Pb collisions, nuclear shadowing is included and binary scaling is applied.

| System | $N_{c\bar{c}/event}$ | $\sigma^{NN}_{c\bar{c}}(mb)$ | $N_{b\bar{b}/event}$ | $\sigma^{NN}_{b\bar{b}}(mb)$ |
|---|---|---|---|---|
| Pb-Pb (5.5 TeV) | 115 | 4.32 | 4.56 | 0.18 |
| p-p (14 TeV) | 0.16 | 11.2 | 0.0072 | 0.51 |

Heavy flavours are produced in the early stage of the collision and, due to their long life-time, they allow to probe the dynamics of the hot and dense system created in heavy ion collisions. In this regard, the study of p-p collisions presents a crucial interest for the interpretation of results obtained in A-A and p-A collisions in order to unravel nuclear effects such as, for instance, shadowing and quenching effects. In particular, the heavy quark energy loss is the object of intense experimental and theoretical researches, after the observation at RHIC of large suppression in the production of high $p_t$ non-photonic electrons. Such an effect has been evidenced, by means of the nuclear modification factor, in central Au + Au collisions at $\sqrt{s_{NN}} = 200$ GeV [8, 9]. In addition, the measurement of charm and beauty production cross sections in p-p collisions at $\sqrt{s} = 14$ TeV should constrain free parameters of NLO pQCD calculations where the theoretical uncertainties on the absolute values are about a factor 2-3 [7]. On the other hand, simulation results indicate that an extrapolation, based on pQCD calculations, can be used to compare charm and beauty cross sections measured in p-p ($\sqrt{s} = 14$ TeV) and in Pb-Pb ($\sqrt{s_{NN}}$ = 5.5 TeV) collisions since the theoretical uncertainty introduced by the extrapolation is about 10% [7].

### A. Open beauty production

In addition to the motivations discussed above, the study of open beauty production in p-p collisions is of particular relevance for understanding bottomonium production in p-p, p-A and A-A collisions. Such a measurement provides the most natural normalization for $\Upsilon$ yields because of similar production processes at the partonic level. The measurement of the $B$ hadron cross section is also mandatory to estimate the contribution of secondary $J/\psi$ (from $B$ decays) to the total $J/\psi$ yield.

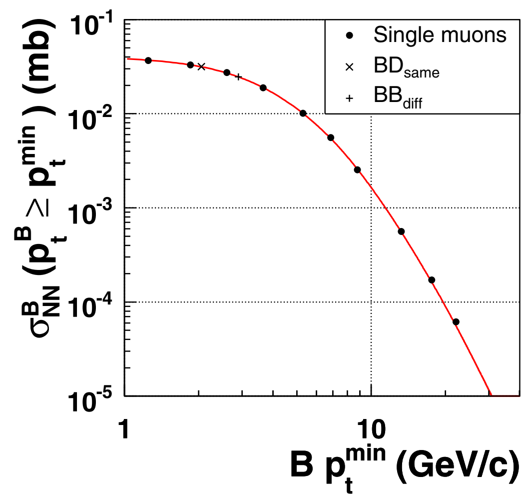


FIG. 1: Differential $B$ hadron inclusive production cross section in central Pb-Pb collisions ($\sqrt{s_{NN}} = 5.5$ TeV) for single muons, low mass unlike-sign dimuons ($BD_{same}$) and high mass unlike-sign dimuons ($BB_{diff}$). The input cross section used in the simulation is also displayed (solid curve). Statistical errors are negligible.

The possibility to determine the differential $B$ hadron inclusive production cross section has been first investigated for central (5%) Pb-Pb collisions at $\sqrt{s_{NN}}$ =

5.5 TeV by means of fast simulations and by using a method developed by the UA1 collaboration in $p - \bar{p}$ collisions [10, 11]. The cross section is determined from the measured single muon $p_t$ distribution as well as from the unlike-sign dimuon yields in the low mass region (each muon originates from the same $B$ meson through a $D$ meson decay, $BD_{same}$) and in the high mass region (each muon comes from the direct decay of a $B$ meson, $BB_{diff}$) [7, 12]. In one data taking period, one expects large statistics of single muons and unlike-sign dimuons from open beauty over a wide $p_t$ and mass range, respectively [12]. Figure 1 shows that the $B$ hadron cross section can be measured up to several tens of GeV/$c$ and that a remarkable agreement between the different channels is achieved.

The preliminary statistics estimate for a nominal p-p run (Table I) is presented in Table IV [13]. In the acceptance of the ALICE muon spectrometer, one expects a large statistics of single muons and unlike-sign dimuons from open beauty. We have also estimated the yields for a reduced sample of events, as it could be collected during the first weeks of data taking at $\sqrt{s} = 14$ TeV, assuming an average luminosity of $10^{30}$ cm$^{-2}$s$^{-1}$ and a data taking time of 200 hours (data sample I). This suggests that the measurement of the single muon $p_t$ distribution can be used to provide a first measurement of the open beauty production cross section at forward rapidities in ALICE.

TABLE IV: Expected yields of single muons and unlike-sign dimuons from open beauty in the ALICE muon spectrometer for p-p collisions at $\sqrt{s} = 14$ TeV. They are shown for a nominal run and for a reduced data sample. See text for details.

| $b \to \mu X$ | $p_t$ (GeV/c) | nominal run | data sample I |
|---|---|---|---|
| | 1.5 - 3 | $8.3 \cdot 10^7$ | $2.0 \cdot 10^6$ |
| | 3 - 6 | $2.6 \cdot 10^7$ | $6.3 \cdot 10^5$ |
| | 6 - 9 | $2.2 \cdot 10^7$ | $5.3 \cdot 10^4$ |
| | 9 - 20 | $4.7 \cdot 10^5$ | $1.1 \cdot 10^4$ |
| $b\bar{b} \to \mu^+\mu^-$ | M (GeV/$c^2$) | nominal run | data sample I |
| | 0.3 - 5 | $7.3 \cdot 10^5$ | $1.8 \cdot 10^4$ |
| | 5 - 20 | $1.2 \cdot 10^5$ | $3.0 \cdot 10^3$ |

Analysis concerning the $B$ hadron production cross section measurement from single muons in p-p collisions at $\sqrt{s} = 14$ TeV, with realistic high statistics simulated data produced within the "Physics Data Challenge" [14], are in progress. Preliminary results have shown that fits to the total muon $p_t$ distribution, with fixed shapes for the different contributing sources and beauty amplitude as the only free parameter, allow to unravel the charm and bottom components in a self-consistent way. As depicted in Fig. 2, in the region $p_t > 3$ GeV/c, where the contribution of muons from $\pi$ and $K$ decay can be neglected and the only background to the beauty signal consists of muons from charm decay, the combined fit gives the muon yield from beauty decay with an accuracy of a few % (about 3%). However, the systematic errors still need to be investigated.

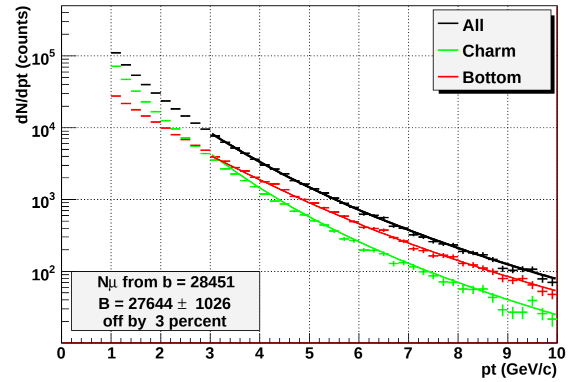


FIG. 2: Transverse momentum distribution of single muons reconstructed in the acceptance of the ALICE muon spectrometer, in p-p collisions at $\sqrt{s} = 14$ TeV (black). Red and green symbols correspond to muons from bottom and charm decay, respectively. The muon contribution from $\pi$ and $K$ decay (not shown) is underestimated in this simulation. The curves show the result of the fit.

In what follows, ongoing studies related to open beauty production are shortly described.

The open beauty production cross section can also be measured by means of $J/\psi$ from $B$ hadron decay. In p-p collisions at 14 TeV, this contribution represents about 22 % (in $4\pi$) of the total $J/\psi$ yield. Feasibility studies [7] have demonstrated the possibility to isolate these secondary $J/\psi$ in p-p collisions by triggering on three-muon events. This component can be identified with a signal to background ratio S/B = 3 and a significance of 80 in a nominal p-p run.

Like-sign correlated muon pairs, which originate in part from $B_0\bar{B}_0$ oscillations, represent another promising channel for the $B$ hadron production cross section measurement. The yield of like-sign correlated muons from beauty decay is here obtained by subtracting the event-mixing distribution from the like-sign distribution [15].

Finally, unlike-sign electron-muon pairs where the electron is identified in the central barrel and the muon is detected in the forward muon spectrometer can be used to extract the same physics information [7, 16]. It is worth to point out that neither a resonance, nor thermal production, nor direct dilepton production can produce correlated electron-muon pairs. It is interesting also to notice that the corresponding signal covers the intermediate rapidity range $-3 < y < -1$, therefore bridging the acceptances of the central and the forward parts of the ALICE detector.

## B. Quarkonium production

The study of quarkonium production should be combined with that of open heavy flavours. The measurement of quarkonia in p-p collisions is of great interest since it is expected to provide information on production mechanisms in a new energy range and it should allow to extract information on parton distribution functions (PDF) at very small Bjorken-$x$ values, down to about $10^{-5}$. It is also the reference for understanding quarkonium production in p-A and A-A collisions and therefore is mandatory for the determination of the nuclear modification factor.

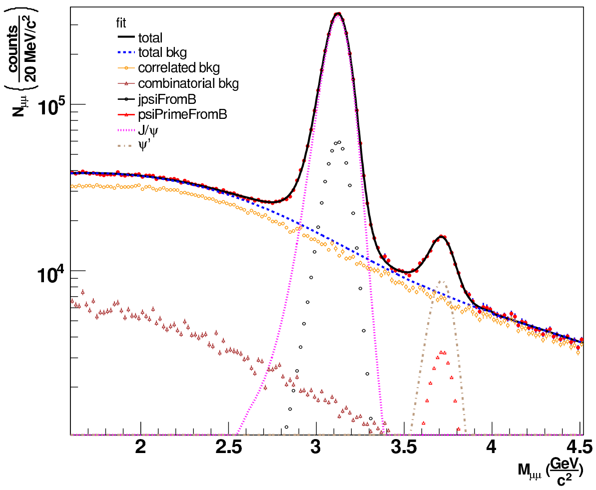


FIG. 3: Invariant mass distribution of unlike-sign dimuons in the acceptance of the ALICE muon spectrometer, in p-p collisions at $\sqrt{s}$ = 14 TeV. The $J/\psi$ mass region is shown.

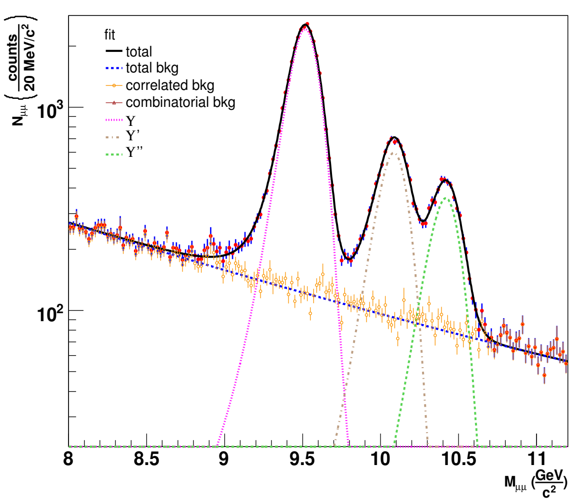


FIG. 4: Invariant mass distribution of unlike-sign dimuons in the acceptance of the ALICE muon spectrometer, in p-p collisions at $\sqrt{s}$ = 14 TeV. The $\Upsilon$ mass region is shown.

The invariant mass of unlike-sign dimuons leads to a direct measurement of quarkonium production. Charmonium and bottomonium production in p-p collisions at $\sqrt{s}$ = 14 TeV has been investigated by means of fast simulations [7, 17]. It is worth to point out that, in the acceptance of the ALICE muon spectrometer, quarkonia can be identified down to $p_t = 0$. The results, corresponding to a standard p-p run, show that charmonium (Fig. 3) and bottomonium states (Fig. 4) are well separated. Note that, in addition to quarkonia, all sources contributing to the unlike-sign dimuon invariant mass continuum have been considered, including muons from correlated and uncorrelated decay of $c\bar{c}$ and $b\bar{b}$ pairs and from decay of $\pi$ and $K$. One can remark that, because of the low multiplicity expected in p-p collisions, the contribution from uncorrelated dimuon sources is negligible.

Table V summarizes the expected yield (S), signal to background ratio (S/B) and significance (S/$\sqrt{\mathrm{S+B}}$) for quarkonia reconstructed in the acceptance of the ALICE muon spectrometer in a nominal p-p run. All quarkonium states are identified with good significance and the corresponding signal to background ratio is always greater than one, except for $\psi'$ (S/B = 0.6). The statistics is very large, in particular for $J/\psi$ (S = $2.8 \cdot 10^6$) and should allow for detailed analysis as a function of rapidity and transverse momentum. In particular, the rapidity dependence of the $J/\psi$ yield should be a relevant observable to unravel PDF at very low Bjorken-$x$ values [17] .

TABLE V: Expected signal (S), signal to background (S/B) and significance (S/$\sqrt{\mathrm{S+B}}$) for quarkonia measured in the acceptance of the ALICE muon spectrometer in a standard p-p run at $\sqrt{s}$ = 14 TeV.

| | S | S/B | S/$\sqrt{\mathrm{S+B}}$ |
|---|---|---|---|
| $J/\psi$ | $2.8 \cdot 10^6$ | 12.0 | 1610 |
| $\psi'$ | $0.075 \cdot 10^6$ | 0.6 | 170 |
| $\Upsilon$(1S) | $27 \cdot 10^3$ | 10.4 | 157 |
| $\Upsilon$(2S) | $6.8 \cdot 10^3$ | 3.4 | 73 |
| $\Upsilon$(3S) | $4.2 \cdot 10^3$ | 2.4 | 55 |

The $J/\psi$ polarization is another promising observable for testing different production mechanisms in p-p collisions [18], since different models predict different behaviours. The $J/\psi$ polarization has been studied from the angular distribution (dN/dcos$\theta$) of positive muons from $J/\psi$ decay, in the helicity frame [19]. The normalized distribution can be parametrized as $1 + \alpha \cos^2\theta$. An unpolarized sample of $J/\psi$ has $\alpha = 0$ while, a positive or negative $\alpha$ value corresponds to a transverse or longitudinal polarization. Recent investigations have demonstrated the capabilities of the ALICE muon spectrometer to measure this observable in p-p collisions [19]. As shown in Fig. 5, the $J/\psi$ polarization can be reconstructed with an uncertainty of a few %.

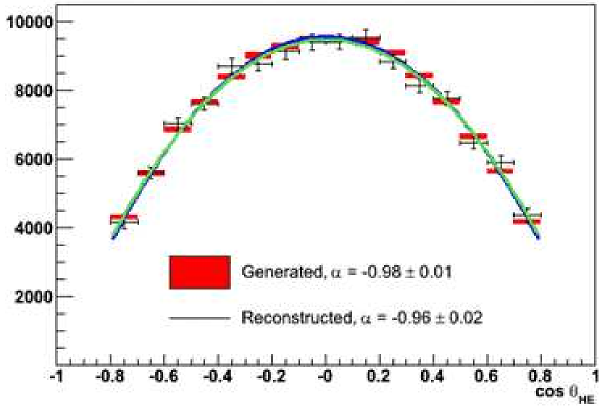


FIG. 5: Angular distribution of $\mu^+$ from $J/\psi$ decay in the helicity frame, for p-p collisions at $\sqrt{s}$ = 14 TeV. The measurement is performed in the domain $p_t$ < 20 GeV/c and $-3.7 < y < -3.3$. Thick and thin symbols correspond to the generated and reconstructed distribution, respectively. The solid line is the result of the fit. See text for details.

## IV. PRODUCTION OF LOW MASS RESONANCES

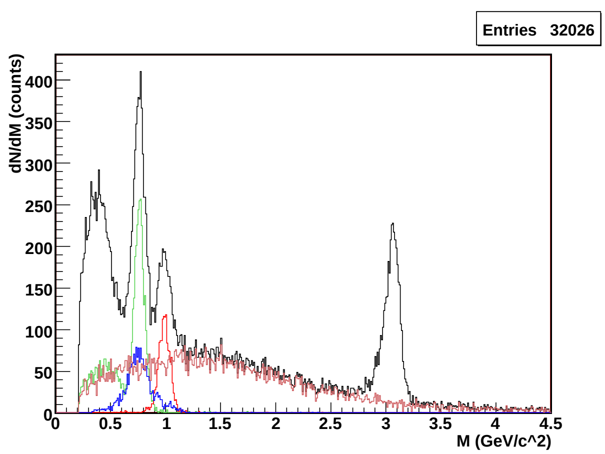


FIG. 6: Invariant mass distribution of unlike-sign dimuons in the acceptance of the ALICE muon spectrometer, in p-p collisions at $\sqrt{s}$ = 14 TeV (black). A transverse momentum cut ($p_t$ > 0.5 GeV/c) is applied on single muons. The contributions from $\omega$ (green), $\rho$ (blue), $\phi$ (red) and open heavy flavours (brown) are shown.

The production of low mass resonances ($\omega$, $\rho$, $\phi$) has been also investigated with the ALICE muon spectrometer. The analysis of full simulations for p-p collisions at $\sqrt{s}$ = 14 TeV, which should provide crucial information for the understanding of A-A collisions, are in progress. The corresponding invariant mass ($M$) distribution of unlike-sign dimuons, measured in the acccceptance of the ALICE muon spectrometer, is presented in Fig. 6 [20]. Note that the muon source from $\pi$ and $K$ decay is underestimated and is negligible in this simulation. A transverse momentum cut of 0.5 GeV/c is applied on single muons. Such a cut results from a compromise between optimization of S/B ratio and acceptance at low $p_t$. In the low invariant mass region ($0.5 < M < 1.5$ GeV/c$^2$), one clearly identifies two peaks attributed to $\omega$ and $\rho$ and, $\phi$ resonances, respectively.

## V. PRODUCTION OF ELECTROWEAK $W^{\pm}$ AND $Z^0$ BOSONS

Massive electroweak $W^{\pm}$ bosons are produced in hard primary collisions. These bosons can decay into muons, mainly in the channel $W^{\pm} \rightarrow \mu^{\pm}\nu_{\mu}$. The dominant process for $W^+$ ($W^-$) production corresponds to a leading order (LO) production and is $u\bar{d}$ ($d\bar{u}$) scattering. In p-p collisions at $\sqrt{s}$ = 14 TeV, $W^{\pm}$ bosons will allow to probe PDF at large $Q^2$ ($Q^2 \sim m_W^2$) in the Bjorken-x range from $\sim 10^{-4}$ to $\sim 10^{-3}$. The measurement of their production yield will permit also to confirm the validity of binary scaling in A-A collisions. Moreover, $W^{\pm}$ boson production could be used as a cross-check of the integrated luminosity measurement.

Figure 7 presents the $p_t$ distribution of single muons in the acceptance of the ALICE muon spectrometer. Charm, beauty and $W^{\pm}$ muonic components have been taken into account. $W^{\pm}$ production exhibits a maximum around 40 GeV/$c$ and dominates the high range of the single muon $p_t$ distribution ($p_t$ > 30 GeV/c). In a nominal p-p run at $\sqrt{s}$ = 14 TeV, more than $5 \cdot 10^5$ $W^{\pm}$ bosons decaying into muons will be produced. This corresponds to about $8.6 \cdot 10^4$ muons in the acceptance of the ALICE muon spectrometer.

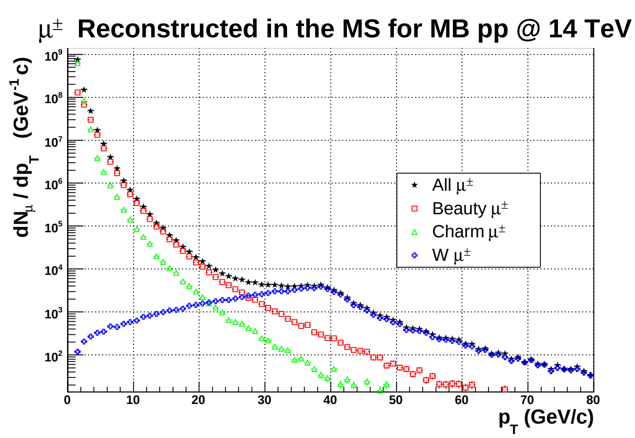


FIG. 7: Transverse momentum distribution of single muons reconstructed in the acceptance of the ALICE muon spectrometer (stars), in p-p collisions at $\sqrt{s}$ = 14 TeV. Squares, triangles and crosses correspond to muons from beauty, charm and $W^{\pm}$ decays, respectively. $Z^0$ production is not simulated.

From the rapidity distributions of $W^{\pm}$, depicted in Fig. 8, one observes that in p-p collisions $W^+$ will be more abundantly produced than $W^-$, therefore leading

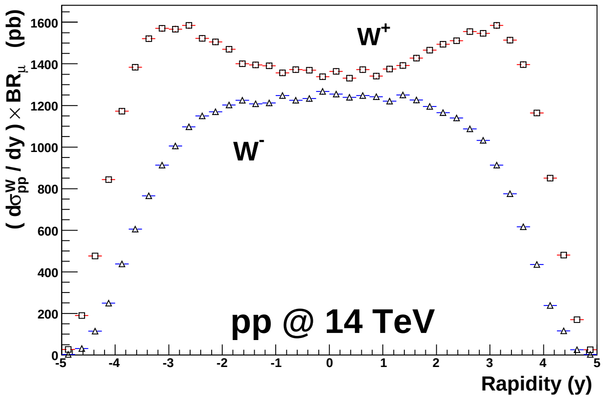


FIG. 8: Rapidity distributions of $W^\pm$ bosons in p-p collisions at $\sqrt{s} = 14$ TeV.

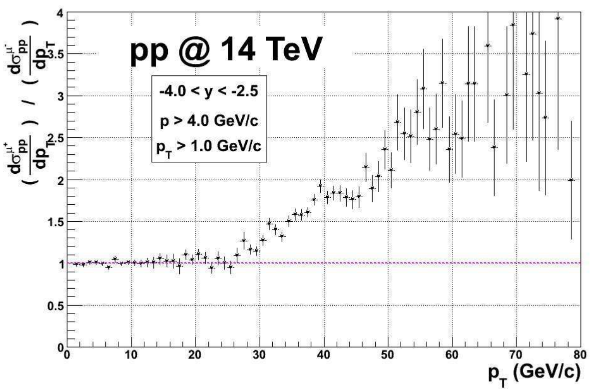


FIG. 9: $N(\mu^+)/N(\mu^-)$ ratio as function of $p_t$ in the acceptance of the ALICE muon spectrometer, in p-p collisions at $\sqrt{s} = 14$ TeV.

to a larger yield of $\mu^+$ than $\mu^-$ [21, 22]. Such an effect is due to the valence quark composition of the colliding system (protons are made up of *uud* valence quarks). It is worth to point out that this asymmetry is more pronounced at the large rapidities corresponding to the acceptance of the muon spectrometer. This is explained by the fact that, in this rapidity region, $W^\pm$ production is dominated by valence quarks.

Figure 9 shows that the $p_t$ dependence of the $N(\mu^+)/N(\mu^-)$ ratio is a promising observable for $W^\pm$ production [21, 22]. Beauty, charm, $W^\pm$ and $Z^0$ contributions are included in the yields. As expected, the $N(\mu^+)/N(\mu^-)$ ratio differs from one for large $p_t$ values ($p_t > 30$ GeV/c), where the muon contribution from $W^\pm$ decay is dominant.

Preliminary studies reveal that $Z^0$ bosons also can be reconstructed in the ALICE muon spectrometer by means of the invariant mass of unlike-sign muon pairs [22]. The estimated yield for one year of data taking is about 2500.

## VI. SUMMARY

An ambitious proton-proton physics program, through a large variety of physics channels, will be carried out with the ALICE muon spectrometer at the LHC. A particular emphasis will be placed on the physics of heavy flavours. The analysis will bring significant insights in a new energy domain and will be an important benchmark for the heavy ion physics. The physics topics are complementary to those addressed by the dedicated proton-proton LHC experiments. In particular, the production of quarkonia will be studied down to very low $p_t$. The detector, which is in its final installation phase, will be ready for operation with first proton beams at $\sqrt{s} = 14$ TeV scheduled in summer 2008. Intensive preparation for data taking and analysis is underway.


[1] F. Carminati et al., ALICE Collaboration, J. Phys. G: Nucl. Part. Phys. **30**, 1517 (2004).
[2] ALICE Collaboration, CERN/LHC **96-21** (1996).
[3] C. Finck for the ALICE Collaboration, J. Phys.: Conf. Series **50**, 397 (2006).
[4] P. Dupieux for the ALICE Collaboration, Ricerca scientifica ed Educazione Permanente, Supplemento **127**, 298 (2007).
[5] F. Guerin et al., ALICE-INT-2006-0002, (2006).
[6] M. Mangano, P. Nason and G. Ridolfi, Nucl. Phys. B **373**, 295 (1992).
[7] B. Alessandro et al., ALICE Collaboration, J. Phys. G: Nucl. Part. Phys. **32**, 1295 (2006).
[8] S.S. Adler et al., Phys. Rev. Lett. **96**, 032301 (2006).
[9] B.I. Abelev et al., Phys. Rev. Lett. **98**, 192301 (2007).
[10] C. Albajar et al., Phys. Lett. B **213**, 405 (1988).
[11] C. Albajar et al., Phys. Lett. B **256**, 121 (1991).
[12] R. Guernane et al., ALICE-INT-2005-018, (2005).
[13] N. Bastid, ECT International Workshop on Heavy Flavor Physics in Heavy Ion Collisions at the LHC (2006).
[14] ALICE Collaboration, CERN-LHCC-2005-018 (2005).
[15] P. Crochet, P. Braun-Munzinger, Nucl. Inst. Meth. A **484**, 564 (2002).
[16] P. Crochet et al., ALICE-INT-2000-01, (2000).
[17] D. Stocco et al., ALICE-INT-2006-029, (2006).
[18] T. Affolder et al., Phys. Rev. Lett. **85**, 2886 (2000).
[19] R. Arnaldi and E. Scomparin, private communication.
[20] F. Nendaz and R. Tieulent, private communication
[21] Z. Conesa del Valle et al., ALICE-INT-2006-021, (2006).
[22] Z. Conesa del Valle for the ALICE Collaboration, Eur. Phys. J. C **49**, 149 (2007).